Electronic supplementary information (ESI)

Tunable Electrical Memory Characteristics by the Morphology of Self-assembled Block Copolymers:PCBM Nanocomposite Films

Jhao-Cheng Chen,[a] Cheng-Liang Liu,[b,*] Ya-Sen Sun,[c,*] Shih-Huang Tung,[d] *and* Wen-Chang Chen[a,d,*]

[a]*Department of Chemical Engineering, National Taiwan University, Taipei 10617, Taiwan.*

E-mail: chenwc@ntu.edu.tw; Tel:+886-2-2362-8398.

[b]*Department of Organic Device Engineering and Research Center for Organic Electronics,*

Yamagata University, Yonezawa, Yamagata 992-8510, Japan. E-mail:

clliu@yz.yamagata-u.ac.jp; Tel:+81-238-26-3309.

[c]*Department of Chemical and Materials Engineering, National Central University, Taoyuan*

32001, Taiwan. E-mail: y*ssun@cc.ncu.edu.tw; Tel:+886-3-422-7151 ext 34205.*

[d]*Institute of Polymer Science and Engineering, National Taiwan University, Taipei, 10617,*

Taiwan.

Electrochemical Properties

The electrochemical properties of **L1** and **L2** were investigated by cyclic voltammetry (CV), as shown in Fig. S2. The p-doping behaviors of **L1** and **L2** films on an ITO-coated glass substrate in supporting electrolyte solution were used to determine HOMO, and LUMO was calculated by the difference between HOMO and optical band gap. The corresponding HOMO energy levels of **L1** and **L2** are -6.00 and -5.92 eV, respectively, while the LUMO levels are -1.51 and -1.41 eV, respectively.
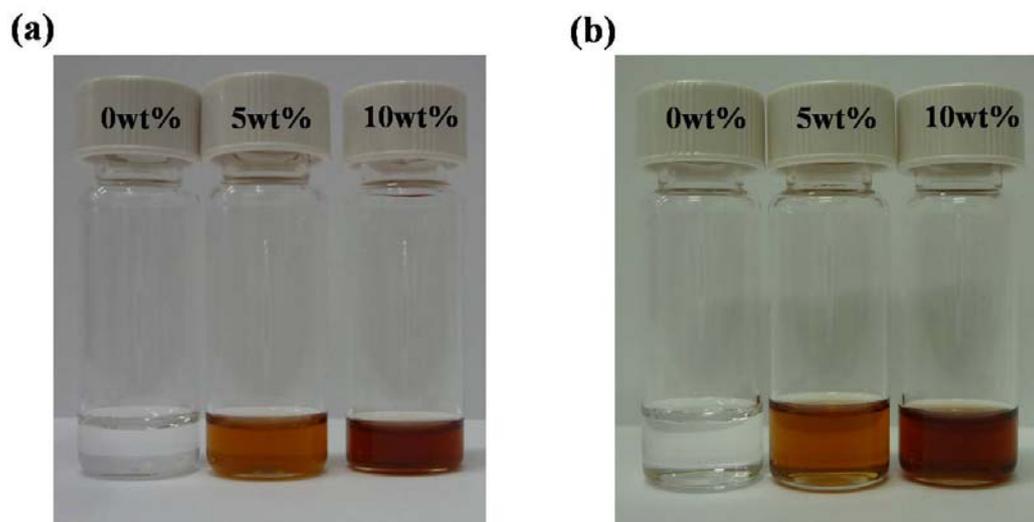
Fig. S1 Photographs of 0%, 5%, 10% (a) PCBM:**L1** and (b) PCBM:**L2** mixtures.
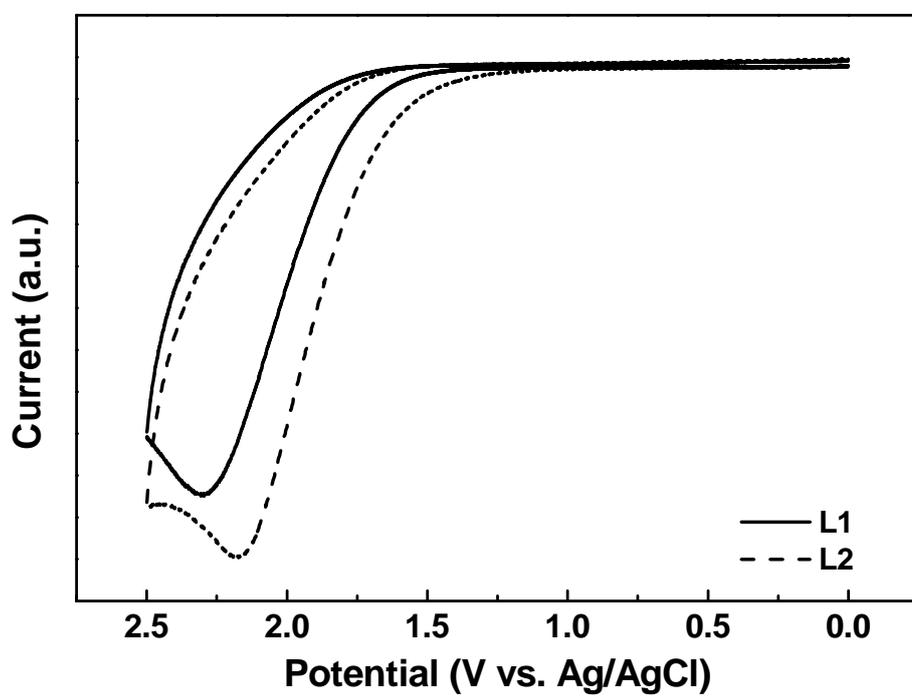
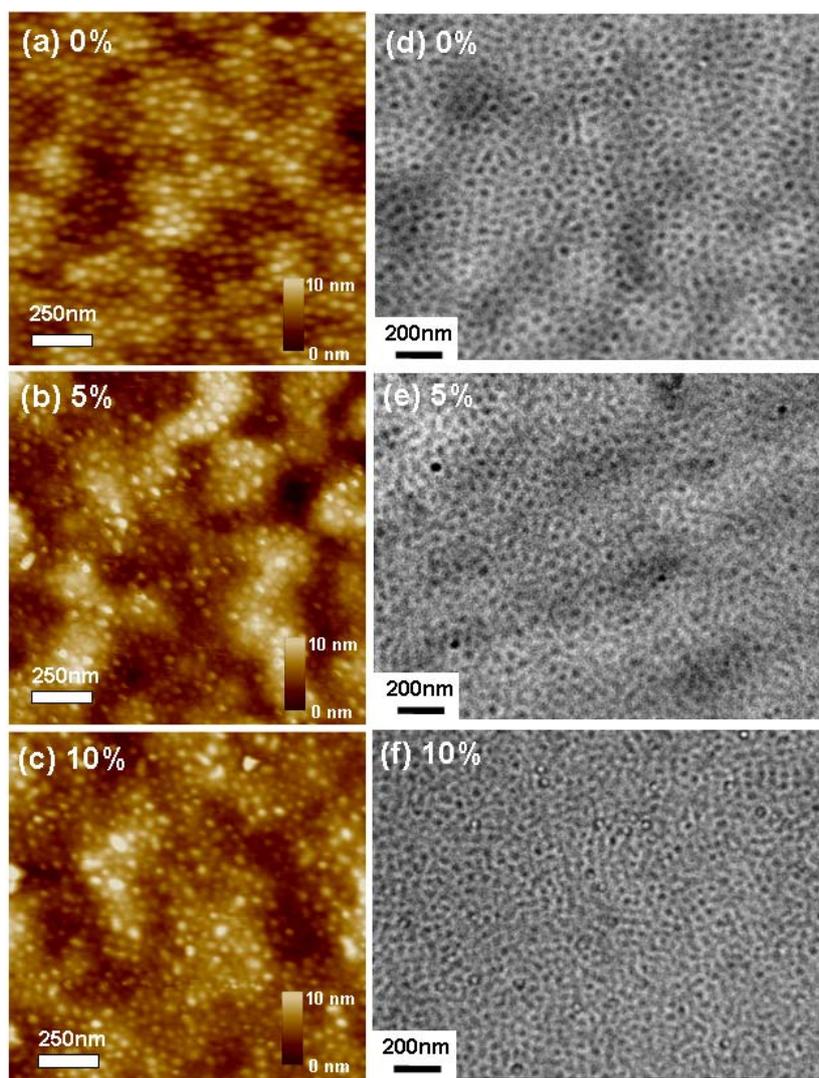**Fig. S2** Cyclic voltammograms of **L1** and **L2** BCP.

Fig. S3 AFM (a-c) height images and TEM (d-f) plane view images of **L1**:PCBM composite

thin films without solvent annealing. The content of PCBM: (a,d) 0%, (b,e) 5% and
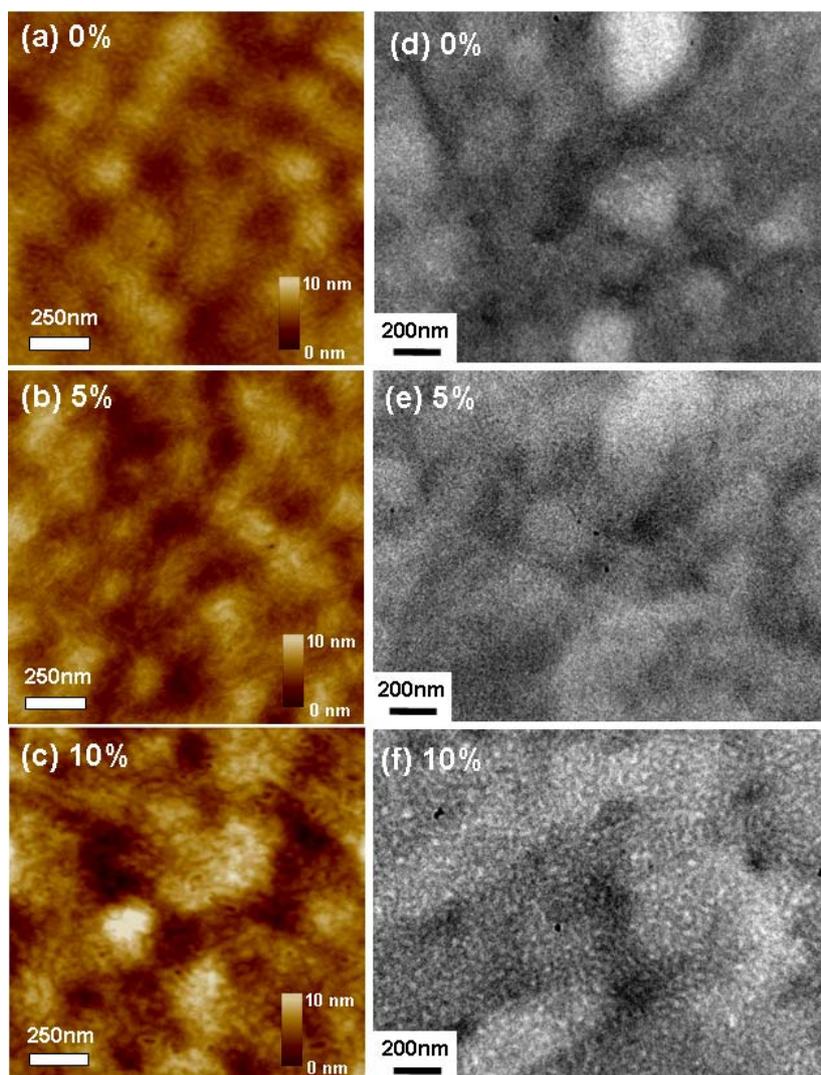
(c,f) 10%.

Fig. S4 AFM (a-c) height images and TEM (d-f) plane view images of **L2**:PCBM composite thin films without solvent annealing. The content of PCBM: (a,d) 0%, (b,e) 5% and (c,f) 10%.
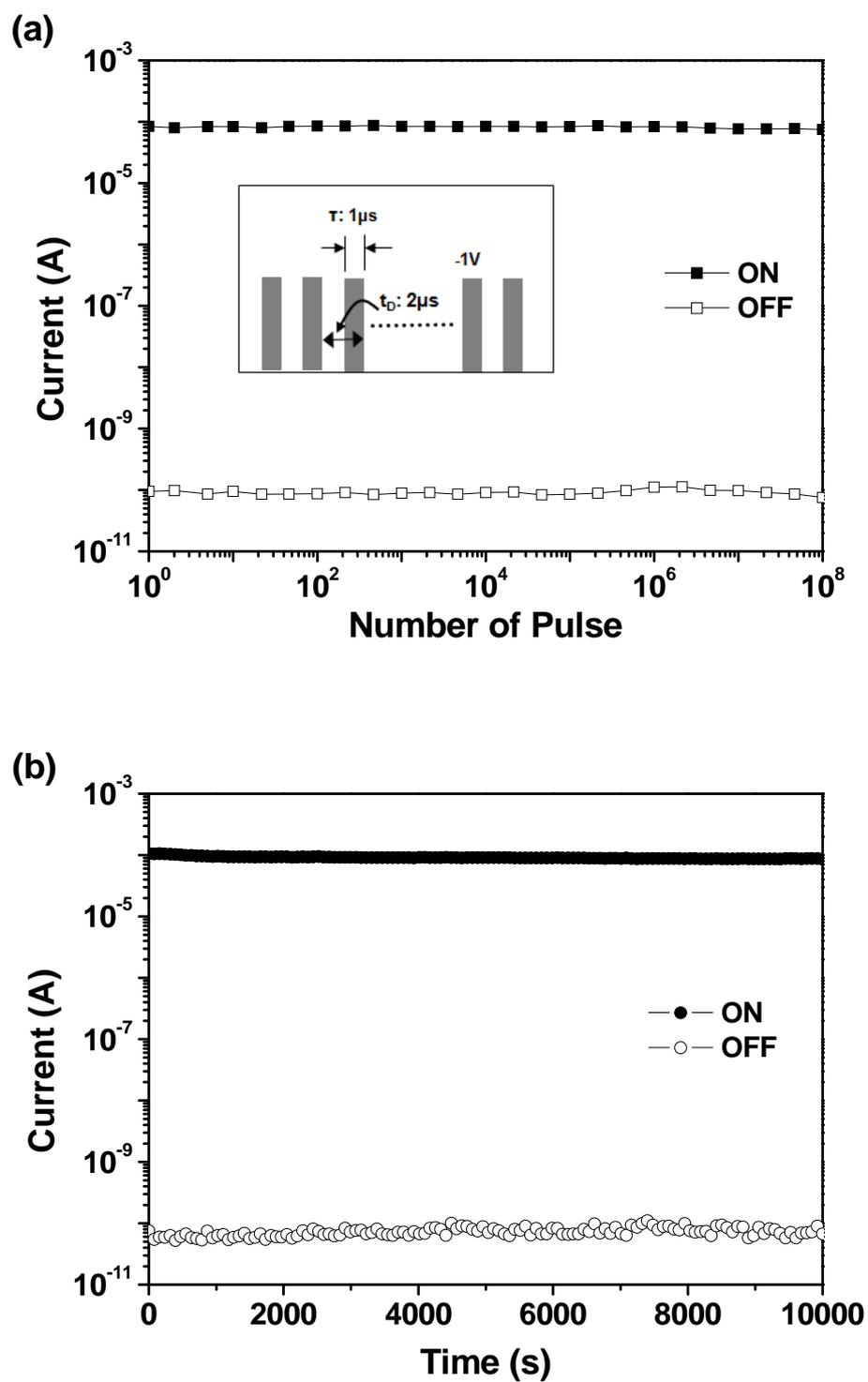
(a)

(b)

Fig. S5 Stability tests for the ITO/5 % PCBM:**L1**/Al device with solvent annealing (a) stimulus effect of read pulses on the ON and OFF states at a read voltage of -1.0 V. The insert shows the pulse shapes in the measurement. (b) retention times on the ON and OFF states under a continuous readout voltage (-1.0 V).
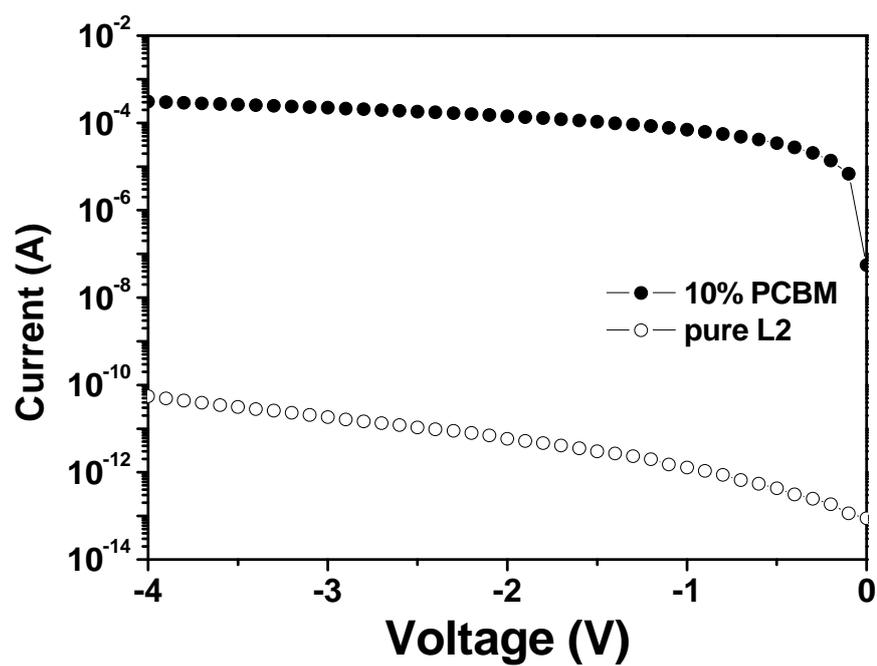
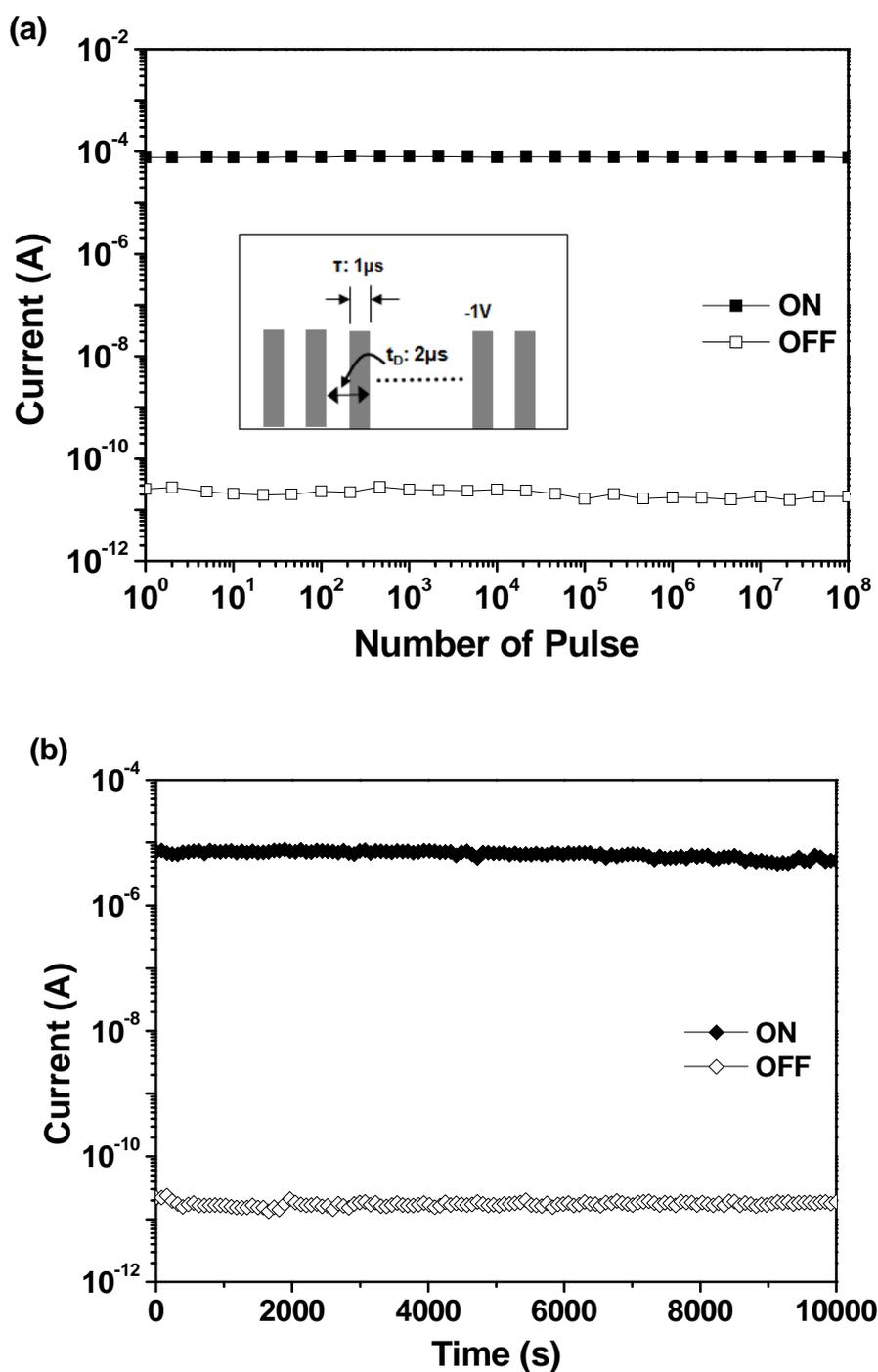**Fig. S6** I-V characteristics of ITO/0% or 10% PCBM:**L2**/Al device with solvent annealing.

Fig. S7 Stability tests for the ITO/5wt% PCBM:**L2**/Al device with solvent annealing (a) stimulus effect of read pulses on the ON and OFF states at a read voltage of -1.0 V. The insert shows the pulse shapes in the measurement. (b) retention times on the ON and OFF states under a continuous readout voltage (-1.0 V).
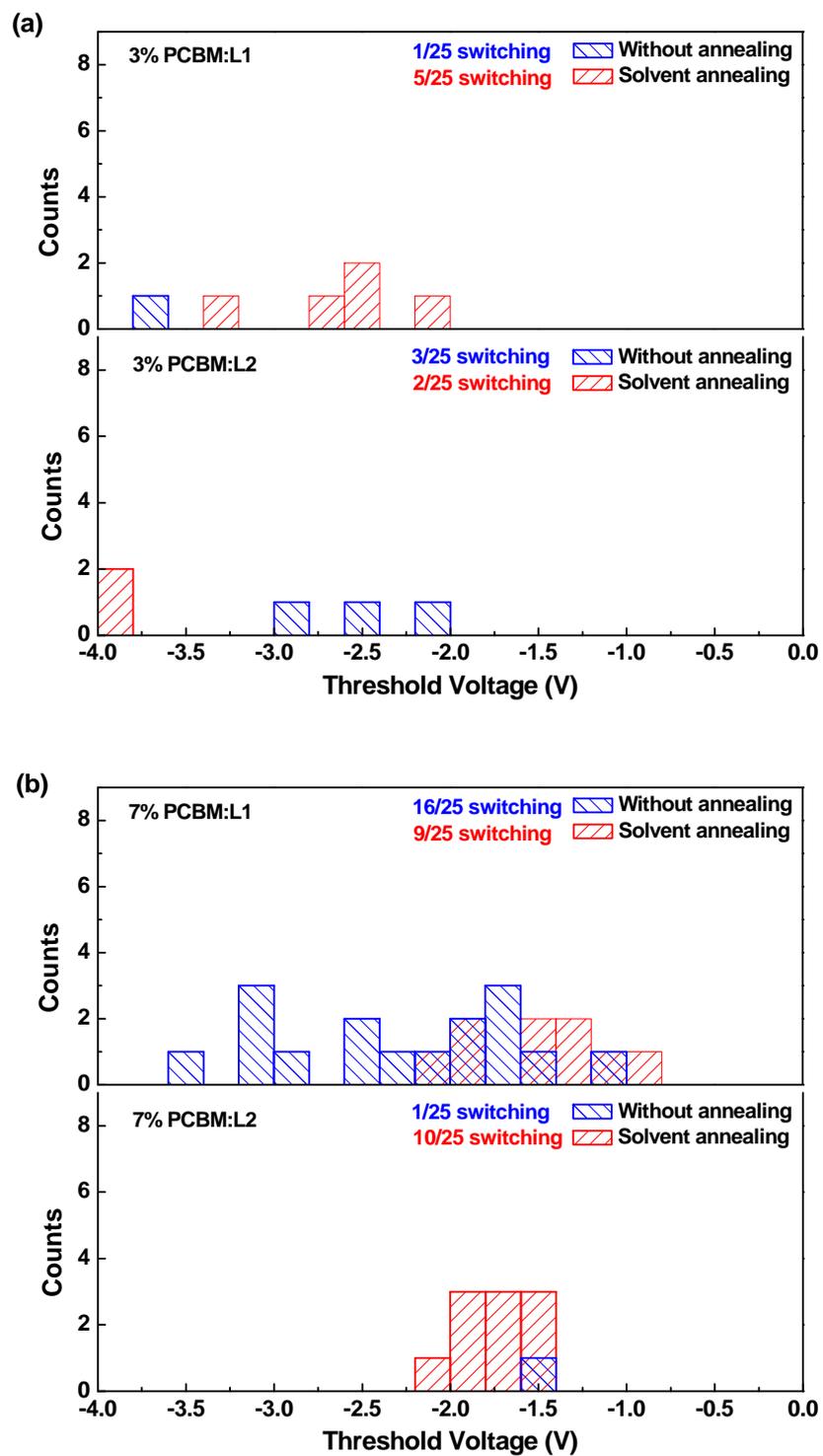
Fig. S8 Threshold voltage distributions of (a) ITO/3% PCBM:**L1** or **L2**/Al device (b) ITO/7% PCBM:**L1** or **L2**/Al device with and without solvent annealing.
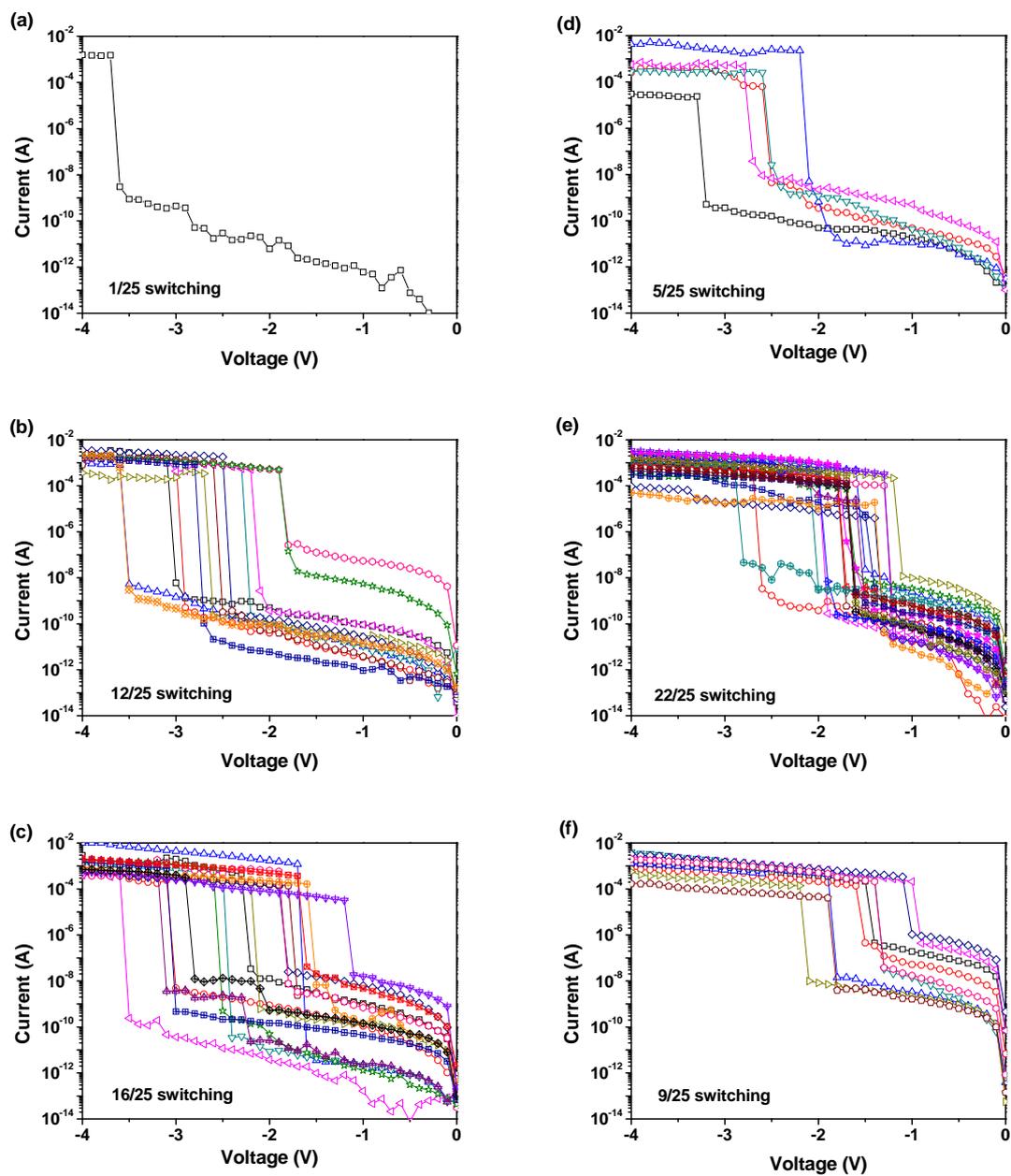
Fig. S9 Switch-ON process based on PCBM:**L1** composite device: (a&d) 3% PCBM (b&e) 5% PCBM (c&f) 7% PCBM; (a,b,c) without solvent annealing (d,e,f) with solvent annealing treatment.

Fig. S10 Switch-ON process based on PCBM:**L2** composite device: (a&d) 3% PCBM (b&e) 5% PCBM (c&f) 7% PCBM; (a,b,c) without solvent annealing (d,e,f) with solvent annealing treatment.
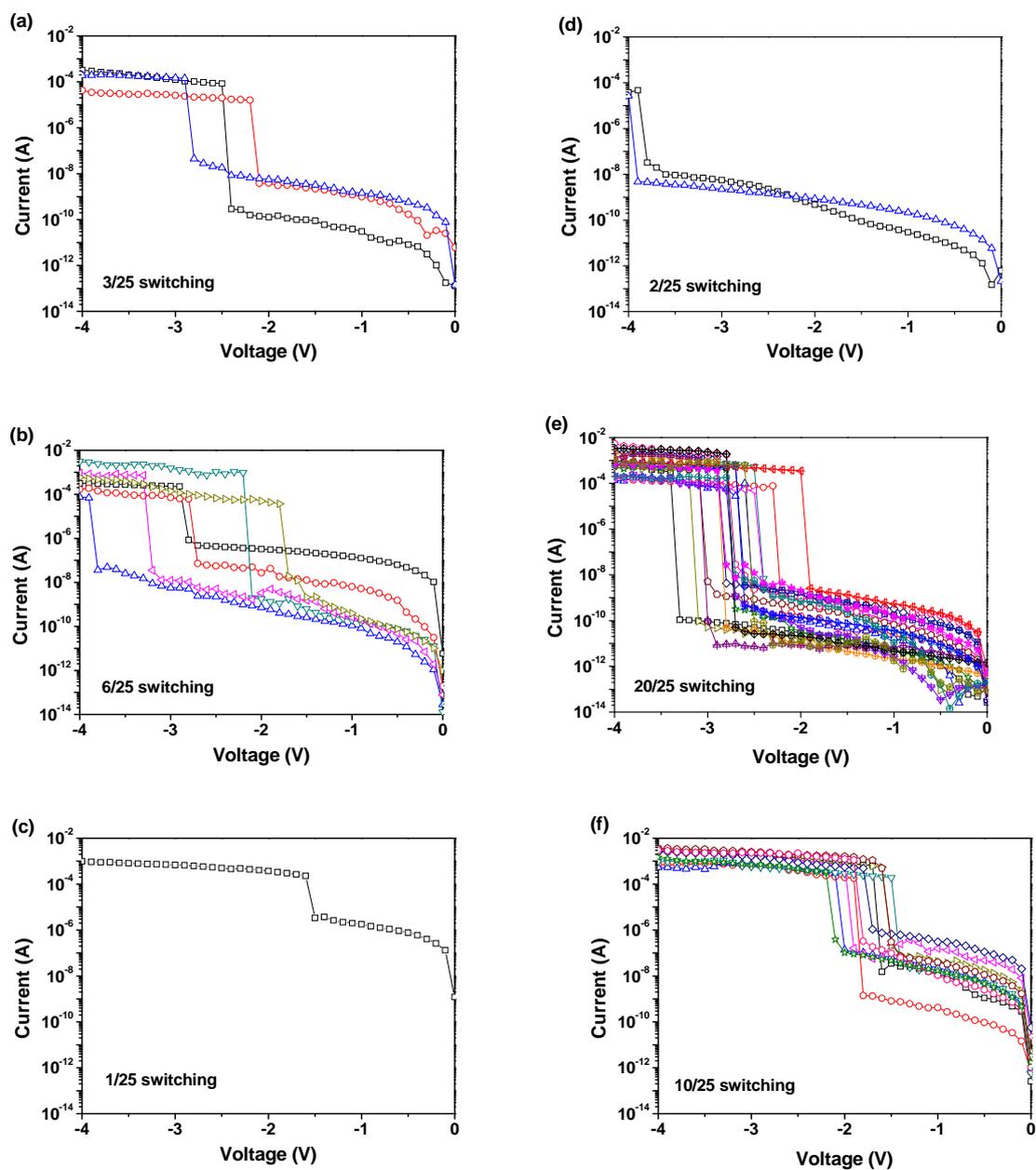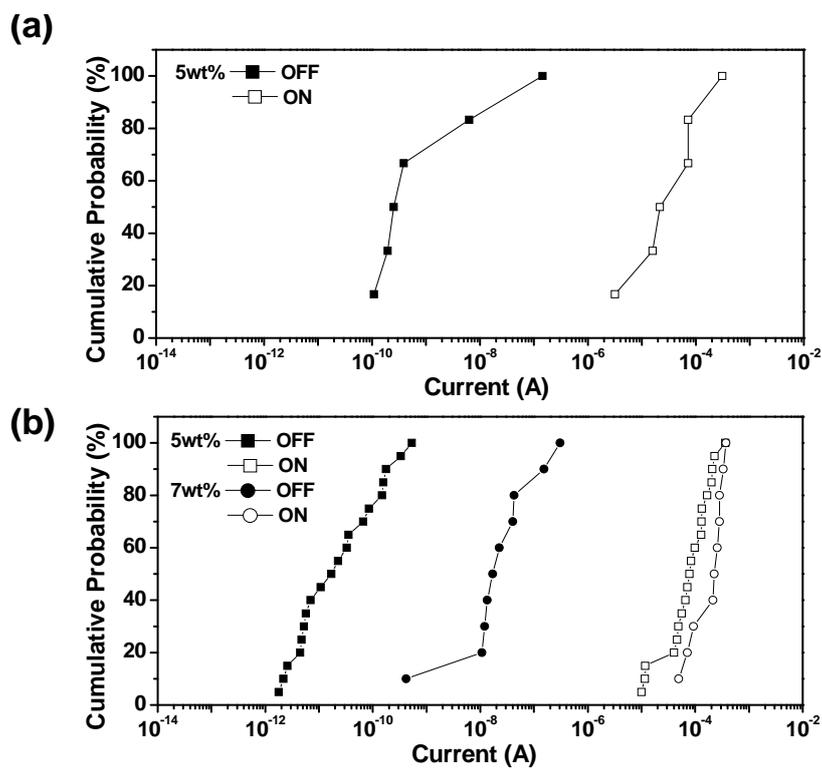
Fig. S11 Cumulative probability data (OFF and ON current at -1.0 V) for PCBM:**L2** composite system (a) without solvent annealing (b) with solvent annealing treatment**.**
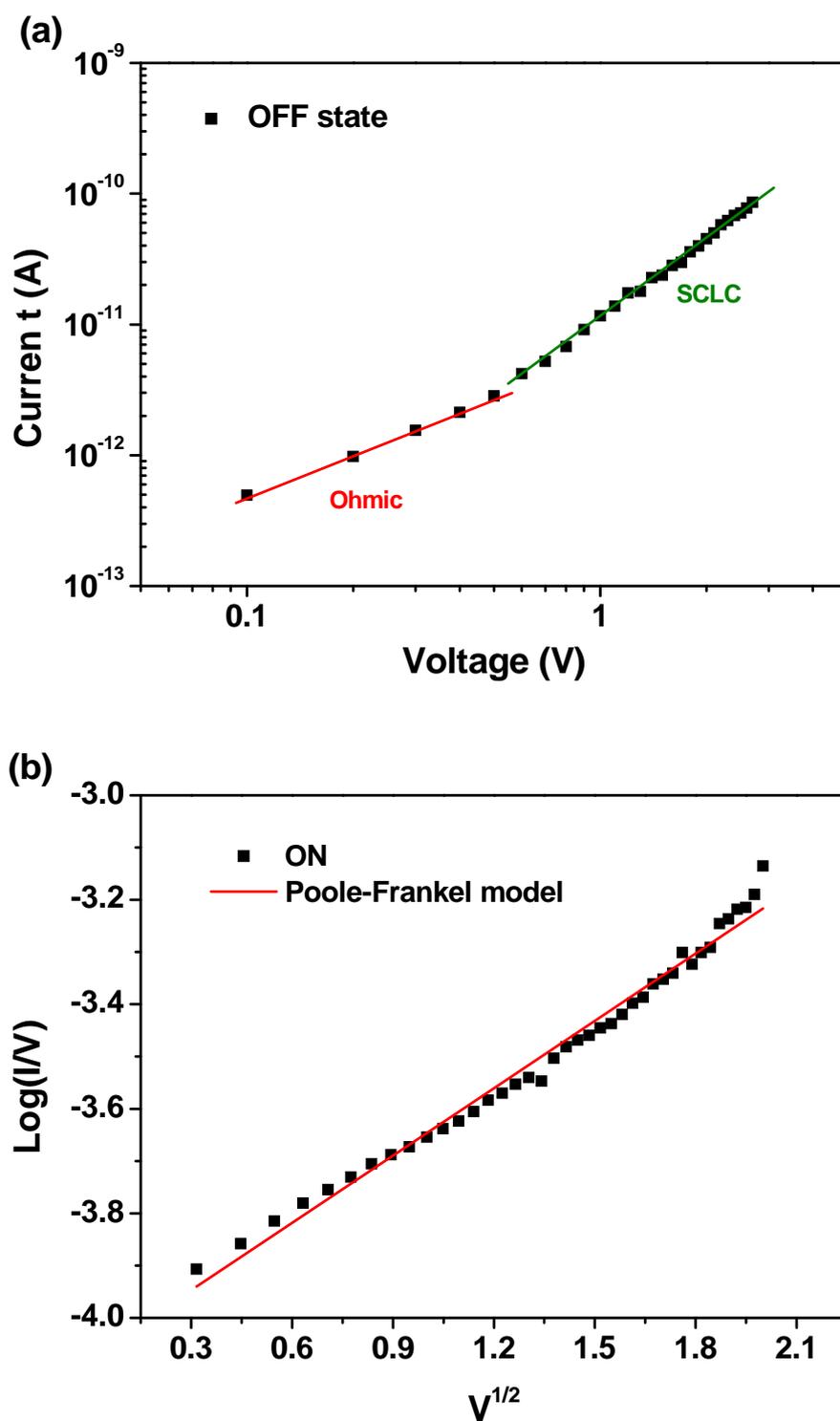
(a) OFF state — Ohmic, SCLC regions; Current (A) vs Voltage (V)

(b) ON — Poole-Frankel model; Log(I/V) vs $V^{1/2}$

Fig. S12 Analysis of I-V characteristics of (a) OFF state and (b) ON state based on ITO/5% PCBM:**L2**/Al device.

Fig. S13 The relative energy levels and conduction mechanism of ITO/BCP:PCBM/Al device.